Groundwater and geothermal anomalies due to a prolate spheroid

Milan HVOŽDARA[1]

[1] Geophysical Institute of the Slovak Academy of Sciences
Dúbravská cesta 9, 845 28 Bratislava, Slovak Republic; e-mail: geofhvoz@savba.sk

Abstract: We present an exact analytical solution of the two potential problems which can help to understand heat flow and groundwater flow in some deep elongated geothermal resources. The thermal conductivity and diffusivity coefficients of the spheroid and surrounding medium are different. The solutions are expressed in terms of the spherical functions of the first and second kinds. The results of numerical calculations are presented for the half-spheroidal body at the surface of the Earth.

Key words: geothermal anomaly model, groundwater flow, potentials of prolate spheroid

1. Introduction

In addition to the solution of the similar problem for the oblate spheroid it is also of interest to determine such a solution for the prolate spheroidal obstacle in the uniform heat or groundwater flow. Similar problems were solved in various potential problems presented e.g. for the D.C. geoelectric potential field *(Cook and Nostrand, 1952; Wait, 1982)*. The magnetic field anomalies can be easily calculated by the modifications of static-electricity problems treated in *Smythe (1968)*. We shall apply similar treatment to the groundwater flow problem. The solution for the groundwater flow was presented for the oblate spheroid in *Hvoždara (2008)*.

We consider the prolate spheroid bounded by rotation of the ellipse with semiaxes a, b ($a > b$) around the vertical axis z which prolongates the longer vertical semiaxis a downward the Earth, as shown in Fig. 1 in section by the x, z plane. The section of this spheroid by the horizontal plane (x, y) is the circle $x^2 + y^2 = b^2$. Let the coefficient of the filtration of the spheroid is κ_T and that of the surrounding medium is κ_1. According to the steady

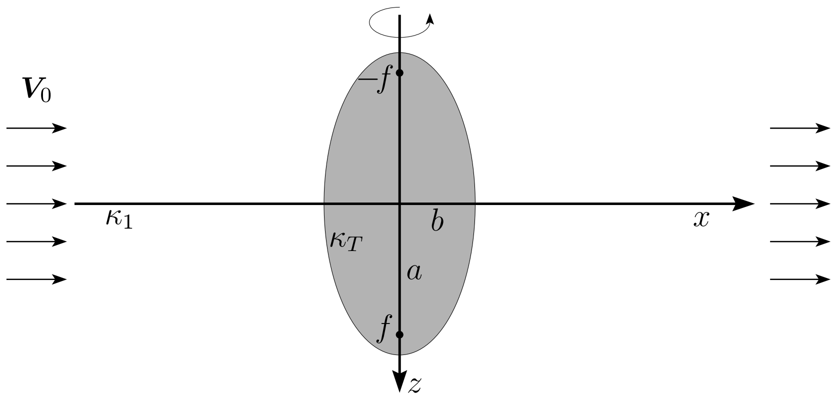

Fig. 1. Model of prolate spheroid rotationally symmetric around vertical z axis.

groundwater flow theory e.g. *Bear and Verruijt (1987)*, the velocity V of the flow can be obtained as the gradient of the potential U:

$$\boldsymbol{V} = -\operatorname{grad} U. \tag{1}$$

The volume flow density across the unit surface area is:

$$\boldsymbol{F} = \kappa \boldsymbol{V}, \quad [\boldsymbol{F}] = (\mathrm{m}^3/\mathrm{s}) \cdot \mathrm{m}^{-2} = \mathrm{m/s}. \tag{2}$$

This represents the volume of groundwater which is transported in 1 second across the $1\,\mathrm{m}^2$ area, so the filtration coefficients κ_1 and κ_T are dimensionless. The velocity field $\boldsymbol{V}$ for the steady laminar flow obeys the equation of continuity in the form:

$$\operatorname{div} \boldsymbol{V} = 0, \tag{3}$$

so the potential U satisfies the Laplace equation

$$\nabla^2 U = 0. \tag{4}$$

The potential of the unperturbed uniform velocity $\boldsymbol{V}_0$ field far from the spheroid is supposed to be of the form

$$U_0(x, y, z) = -V_0(x \cos\varphi_0 + y \sin\varphi_0), \tag{5}$$

where φ_0 is azimuth of $\boldsymbol{V}_0$ reckoned to the x-axis. The presence of spheroidal obstacle causes perturbation potential $U_1^*(x,y,z)$ outside of the spheroid which also obeys the Laplace equation as well as the potential $U_T(x,y,z)$ inside the spheroid. On the surface S of the spheroid, continuity of the potentials and normal volume flow density must be fulfilled:

$$[U_0 + U_1^*]_S = [U_T]_S\,, \tag{6}$$

$$\kappa_1 \left[\frac{\partial}{\partial n}\left(U_0 + U_1^*\right)\right]_S = \kappa_T \left[\frac{\partial}{\partial n} U_T\right]_S . \tag{7}$$

We will solve this boundary value problem by the method of separation of variables in the prolate spheroidal system (α, β, φ). The transformation relations to the Cartesian system are:

$$x = f \operatorname{sh}\alpha \sin\beta \cos\varphi, \quad y = f \operatorname{sh}\alpha \sin\beta \sin\varphi, \quad z = f \operatorname{ch}\alpha \cos\beta \tag{8}$$

(see e.g. *Lebedev (1963), Arfken (1966), Madelung (1957)*). The coordinates α, β, φ vary over the intervals:

$$\alpha \in \langle 0, +\infty), \;\; \beta \in \langle 0, \pi\rangle, \;\; \varphi \in \langle 0, 2\pi),$$

and f is the prolateness parameter

$$f = \sqrt{a^2 - b^2}, \tag{9}$$

where a, b are the lengths of the major or minor semiaxes, respectively, of the generating vertical ellipse (see Fig. 1). Using transformation relations (8) we can find that surfaces $\alpha =$ const. are z-prorated rotational ellipsoids defined by equations:

$$\frac{x^2 + y^2}{f^2 \operatorname{sh}^2\alpha} + \frac{z^2}{f^2 \operatorname{ch}^2\alpha} = 1 \quad \text{or} \quad \frac{r^2}{f^2 \operatorname{sh}^2\alpha} + \frac{z^2}{f^2 \operatorname{ch}^2\alpha} = 1, \tag{10}$$

where $r = \sqrt{x^2 + y^2}$ is the horizontal distance from z-axis. The equation of ellipse in (x, z) plane which generates the surface of the z-prolate spheroid S is:

$$\frac{x^2}{b^2} + \frac{z^2}{a^2} = 1. \tag{11}$$

This is matched with the supporting spheroid $\alpha = \alpha_0$ if we put in (10):

$$a^2 = f^2 \operatorname{ch}^2\alpha_0, \quad b^2 = f^2 \operatorname{sh}^2\alpha_0. \tag{12}$$

We know that there holds

$$\operatorname{ch}^2\alpha_0 - \operatorname{sh}^2\alpha_0 = 1, \tag{13}$$

so we easily find the prolateness parameter f:

$$f^2 = a^2 - b^2, \quad f = \sqrt{a^2 - b^2}, \tag{14}$$

which means that f is numerical eccentricity of the generating ellipse with foci in the points on z-axis: $(0, 0, -f), (0, 0, +f)$. The polar axis for the angle β is halfline $z \in \langle 0, +\infty)$, which corresponds to $\beta = 0$, and the halfline $z \in (-\infty, 0\rangle$ which corresponds to $\beta = \pi$. We obtain the coordinate surfaces $\beta = \text{const}$ from (8) eliminating $\operatorname{ch}\alpha$ and $\operatorname{sh}\alpha$ by using (13). These are confocal hyperboloids

$$\frac{z^2}{f^2 \cos^2\beta} - \frac{r^2}{f^2 \sin^2\beta} = 1. \tag{15}$$

We note that the plane $z = 0$ corresponds to a degenerated hyperboloid $\beta = \pi/2$. From relations (12) we obtain:

$$\mathrm{e}^{\alpha_0} = (a + b)/f, \quad \alpha_0 = \ln[(a + b)/f]. \tag{16}$$

In this manner we link the spheroidal system (α, β, φ) to the generating ellipse. We also record the Lame's metrical parameters from *Lebedev (1963)*:

$$h_\alpha = f(\operatorname{sh}^2\alpha + \sin\beta)^{1/2} = h_\beta, \quad h_\varphi = f \operatorname{sh}\alpha \sin^2\beta. \tag{17}$$

The particular solution of the Laplace equation in the prolate ellipsoidal system can be found e.g. in *Lebedev (1963)*. This is a combination of functions:

$$U_{nm}(\alpha, \beta, \varphi) = \begin{Bmatrix} P_n^m(\operatorname{ch}\alpha) \\ Q_n^m(\operatorname{ch}\alpha) \end{Bmatrix} P_n^m(\cos\beta) \begin{Bmatrix} \cos m\varphi \\ \sin m\varphi \end{Bmatrix}. \tag{18}$$

Here $P_n^m(s), Q_n^m(s)$ are the associated spherical functions for argument $s = \operatorname{ch}\alpha > 1, P_n^m(\cos\beta)$ are the associated Legendre functions of degree n, order m:

$$P_n^m(\eta) = (1 - \eta^2)^{m/2} \, \frac{\mathrm{d}^m P_n(\eta)}{\mathrm{d}\,\eta^m}. \tag{19}$$

From the theory of spherical functions we know that spherical functions of the second kind $Q_n^m(s)$ are singular for $s \to 1$, so in the interior potential $U_T(\alpha, \beta, \varphi)$ cannot be applied. The unperturbed potential field U_0 given by (5) can be written in the form:

$$U_0(r, \varphi) = -V_0 r \cos(\varphi - \varphi_0) = -V_0 f \,\mathrm{sh}\,\alpha \sin\beta \cos(\varphi - \varphi_0). \tag{20}$$

We know that $\sin\beta = P_1^1(\cos\beta)$, and from the orthogonality of the spherical functions as well as from the Fourier series of functions $\cos m\varphi, \sin m\varphi$ we can state that only solutions with $n = 1$ and $m = 1$ will appear in our problem. Then the potential inside the ellipsoid is:

$$U_T = -V_0 B_1 f \,\mathrm{sh}\,\alpha \sin\beta \cos(\varphi - \varphi_0), \tag{21}$$

which is multiple of the primary potential (20) since $P_1^1(\mathrm{ch}\,\alpha) = \mathrm{sh}\,\alpha$. Outside the spheroid we take the potential as the sum of $U_0(\alpha, \beta, \varphi)$ and perturbation part with function $Q_1^1(\mathrm{ch}\,\alpha)$:

$$U_1 = -V_0 f \left[\mathrm{sh}\,\alpha + A_1 Q_1^1(\mathrm{ch}\,\alpha)\right] \sin\beta \cos(\varphi - \varphi_0). \tag{22}$$

The functions $P_1^1(\mathrm{ch}\,\alpha)$ cannot occur in U_1 since these are singular for $\mathrm{ch}\,\alpha \to +\infty$. We determine the coefficients A_1, B_1 by using the boundary conditions (6) and (7) on the spheroid $\alpha = \alpha_0$:

$$[U_1]_{\alpha_0} = [U_T]_{\alpha_0}, \quad [\partial U_1/\partial\alpha]_{\alpha_0} = (\kappa_T/\kappa_1) [\partial U_T/\partial\alpha]_{\alpha_0}. \tag{23}$$

We easily obtain the following relations:

$$B_1 \,\mathrm{sh}\,\alpha_0 = A_1 Q_1^1(\mathrm{ch}\,\alpha_0) + \mathrm{sh}\,\alpha_0, \tag{24}$$

$$\frac{\kappa_T}{\kappa_1} B_1 \,\mathrm{ch}\,\alpha_0 = \left[\mathrm{ch}\,\alpha_0 + A_1 \,\mathrm{sh}\,\alpha_0 Q_1^1(\mathrm{ch}\,\alpha_0)\right]. \tag{25}$$

Elimination method of solution will give:

$$A_1 = \frac{(\kappa_T/\kappa_1 - 1)\,\mathrm{ch}\,\alpha_0 \,\mathrm{sh}\,\alpha_0}{\mathrm{sh}^2\alpha_0\, Q_1^1(\mathrm{ch}\,\alpha_0) - (\kappa_T/\kappa_1)\,\mathrm{ch}\,\alpha_0\, Q_1^1(\mathrm{ch}\,\alpha_0)}, \tag{26}$$

$$B_1 = 1 + Q_1^1(\mathrm{ch}\,\alpha_0) A_1/\,\mathrm{sh}\,\alpha_0. \tag{27}$$

In (25) we have used: $\mathrm{d}\,Q_1^1(\operatorname{ch}\alpha_0)/\,\mathrm{d}\,\alpha = \operatorname{sh}\alpha\, Q_1^{1'}(\operatorname{ch}\alpha_0)$. It is necessary to quote expressions for functions $Q_1^1(s)$ and its derivatives since these are not very frequent. In *Lebedev 1963* we find the following expressions valid for $s > 1$:

$$Q_1(s) = \sum_{k=0}^{\infty} \frac{1}{2k+3}\,\frac{1}{s^{2k+2}} = (s/2)\ln\frac{s+1}{s-1} - 1. \tag{28}$$

$$Q_1^1(s) = (s^2-1)^{1/2}\,\frac{\mathrm{d}}{\mathrm{d}\,s}\,Q_1(s) = -(s^2-1)^{1/2}\sum_{k=0}^{\infty}\frac{(2k+2)}{(2k+3)}\,\frac{1}{s^{2k+3}} =$$
$$= (s^2-1)^{1/2}\left\{\frac{1}{2}\ln\frac{s+1}{s-1} - \frac{s}{s^2-1}\right\}. \tag{29}$$

The expression for $Q_1^{1'}(s)$ can be derived from (29). It is obvious that $Q_1^1(s)$ and its derivative converge to zero for $s \to +\infty$ which implies zero values of the perturbing potential $U_1^*(\alpha,\beta,\varphi)$ far from the spheroid.

2. Calculations for the half-spheroidal obstacle

It is clear that the presented solution can be easily adapted also for the half-spheroidal obstacle which touches the earth surface plane $z = 0$. This seems to be more applicable for hydro-geothermal problems. Additional condition for the velocity field is a zero value of the z-derivative of potentials U_1 and U_T which guaranties that there is no outflow across for the plane $z = 0$. This condition corresponds to zero value of the β derivative of potentials U_1 and U_T on the surface $\beta = \pi/2$. This is clearly satisfied, because both these potentials are proportional to $\sin\beta$, with β-derivative equal to $\cos\beta$. We calculate the velocity field separately for the interior and exterior of the half-spheroid. In the interior we have the potential

$$U_T(\alpha,\beta,\varphi) = -B_1 V_0 f \operatorname{sh}\alpha \sin\beta\cos(\varphi-\varphi_0), \tag{30}$$

where coefficient B_1 is given by (27). Using transformation relations (8) we easily obtain the expression for U_T in Cartesian coordinates:

$$U_T(x,y,z) = -B_1 V_0 (x\cos\varphi_0 + y\sin\varphi_0). \tag{31}$$

This is a well-known potential of uniform velocity field in the (x, y) plane of azimuth φ_0 modified by the factor B_1. The components of velocity are:

$$V_T x = B_1 V_0 \cos\varphi_0, \quad V_T y = B_1 V_0 \sin\varphi_0, \quad V_T z = 0. \tag{32}$$

The velocity outside the half-spheroid is clearly the sum of the exciting velocity field V_0 and additional V_1^* which must be calculated from the curvilinear components

$$V_{1\alpha}^* = -\frac{1}{h_\alpha}\frac{\partial U_1^*}{\partial\alpha},\ V_{1\beta}^* = -\frac{1}{h_\beta}\frac{\partial U_1^*}{\partial\beta},\ V_{1\varphi}^* = -\frac{1}{h_\varphi}\frac{\partial U_1^*}{\partial\varphi}, \tag{33}$$

where the anomalous potential is:

$$U_1^*(\alpha, \beta, \varphi) = -V_0 A_1 Q_1^1(\operatorname{sh}\alpha)\sin\beta\cos(\varphi - \varphi_0). \tag{34}$$

Lame's metrical parameters are given by formulae (10). The curvilinear components of $\operatorname{grad} U_1^*$ can be easily calculated and for the Cartesian components we use the transformation relations using formulae:

$$\begin{aligned}
V_x^* &= V_r^* \cos\varphi - V_\varphi^* \sin\varphi, \quad V_y^* = V_r^* \sin\varphi - V_\varphi^* \cos\varphi, \\
V_z^* &= \left[-V_\beta^* \operatorname{ch}\alpha \sin\beta + V_\alpha^* \operatorname{sh}\alpha\cos\beta\right]\left[\operatorname{sh}^2\alpha + \sin^2\beta\right]^{-1/2}, \\
V_r^* &= \left[V_\beta^* \operatorname{sh}\alpha\cos\beta + V_\alpha^* \operatorname{ch}\alpha\sin\beta\right]\left[\operatorname{sh}^2\alpha + \sin^2\beta\right]^{-1/2}.
\end{aligned} \tag{35}$$

Here we adopt the formulae from *Madelung (1957)* with substitutions $(v, u, \varphi) \to (\alpha, \beta, \varphi)$ and $u = \pi/2 - \beta$, and Madelung's $a_u = -V_\beta$ because the direction of his unit vector $\boldsymbol{e}_u$ is opposite to our $\boldsymbol{e}_\beta$. Now we have a complete set of formulae to prepare a program code for numerical calculations. We need perform the calculations in the network of (x, z) or (x, y) coordinates. Then it is necessary to present calculations for prolate spheroidal coordinates (α, β, φ) $\operatorname{sh}\alpha, \operatorname{ch}\alpha$ at given x, y, z. We know that the section of coordinate surface $\alpha = \text{const}$ is an ellipse given by the equation (10) in (r, z) plane; their foci are in points $z = \pm f$, its z-axis major (vertical) semiaxis is equal to $f\operatorname{ch}\alpha$ and minor semiaxis (horizontal) is equal to $f\operatorname{sh}\alpha$. Using the knowledge from analytical geometry we find that for every (r, z) point on this ellipse the sum of distances from the first and second focus must be equal to the doubled value of major semiaxis, which is $2f\operatorname{ch}\alpha$. It holds:

$$\left[r^2+(z-f)^2\right]^{1/2}+\left[r^2+(z+f)^2\right]^{1/2}=2f\,\mathrm{ch}\,\alpha, \tag{36}$$

where $r^2 = x^2 + y^2$. Using this equation we easily assign $\mathrm{ch}\,\alpha$ to x, y, z values, since $f = \sqrt{a^2 - b^2}$ is a constant given by the principal ellipse of the prolate spheroid, which creates a whole family of confocal ellipses $\alpha = \text{const}$. We determine the $\mathrm{sh}\,\alpha$ value to be

$$\mathrm{sh}\,\alpha=\left[\mathrm{ch}^2\alpha-1\right]^{1/2} \quad \text{and} \quad \mathrm{e}^{\alpha}=\mathrm{ch}\,\alpha+\mathrm{sh}\,\alpha. \tag{37}$$

Using (8) the angle coordinate β is given by:

$$\cos\beta = z/(f\,\mathrm{ch}\,\alpha). \tag{38}$$

For points on the semiaxis $z > 0$ there is $r = 0$ and from (36) we have:

$$|z-f|+|z+f|=2f\,\mathrm{ch}\,\alpha. \tag{39}$$

If $z > 0$, $r = 0$ and if $z > f$ we have from this relation:

$$2z = 2f\,\mathrm{ch}\,\alpha, \tag{40}$$

which gives $\mathrm{ch}\,\alpha = z/f$ and $\beta = 0$. But on this focal segment $z \in \langle -f, f\rangle$ there is clearly $\mathrm{ch}\,\alpha = 1, \mathrm{sh}\,\alpha = 0$ and the angle β can be calculated using the relation

$$\cos\beta = z/f. \tag{41}$$

For the azimuthal angle φ we have the well-known relation:

$$\mathrm{tg}\,\varphi = y/x, \qquad \varphi \in \langle 0, 2\pi) \tag{42}$$

for all space. For our numerical calculations we have checked various parameters of the prolate half-spheroidal obstacle at the surface of the earth. Here we present the isoline and profile curves for the spheroid with dimensions of semiaxes $a = 10\,\mathrm{m}$, $b = 4\,\mathrm{m}$ which gives the eccentricity $f = \sqrt{a^2 - b^2} = 9.165\,\mathrm{m}$ and the generating ellipse is vertical as shown Fig. 1. We put the filtration coefficients ratio $\kappa_T/\kappa_1 = 2$ for highly porous (penetrable) obstacle or $\kappa_T/\kappa_1 = 0.2$ for weakly penetrable obstacle. We put the unperturbed velocity value $V_0 = 1\,\mathrm{m/s}$ which is unrealisticly high for real groundwater in sedimentary basins, but the presented results (graphs)

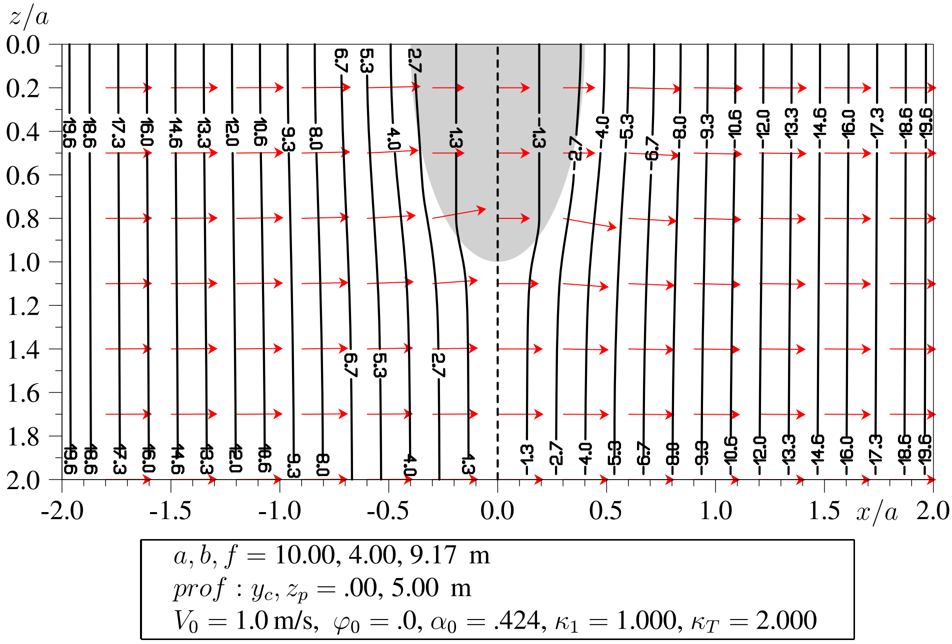

Fig. 2a. Potential isolines around the penetrable prolate hemispheroidal obstacle and velocity arrows.

can be easily matched to smaller values of V_0 e.g. $V_0 = 0.01$ m/s. In series of Figs 2a–d we present the isoline results for the central plane $y_c = 0$ and profile curves are plotted for the depth $z_p = a/2$ (5 m), which corresponds to some interior z-plane in the halfspace and halfspheroid. In Fig. 2a we present isolines of the perturbing velocity potential. We can see that the velocity arrows tend to the interior of the halfspheroid, especially for depths $z/a > 0.5$. In Fig. 2b there are presented isolines of the anomalous velocity potential $U^*(x, y, z)$ in the vertical plane x, z and $y = y_c = 0$ and also its profile curve for $z_p/a = 0.5$. In the next Figs 2c,d the maps for vertical (V_z) and horizontal (V_x) components of the velocity are shown. We can see that the vertical component of the velocity attains the negative values on the left ($x < -b$) of the halfspheroid which means outflow to the surface $z = 0$, while for ($x > b$) we have positive values of V_z. The horizontal component grows by about 23.5% on the left boundary of the spheroid, while inside the

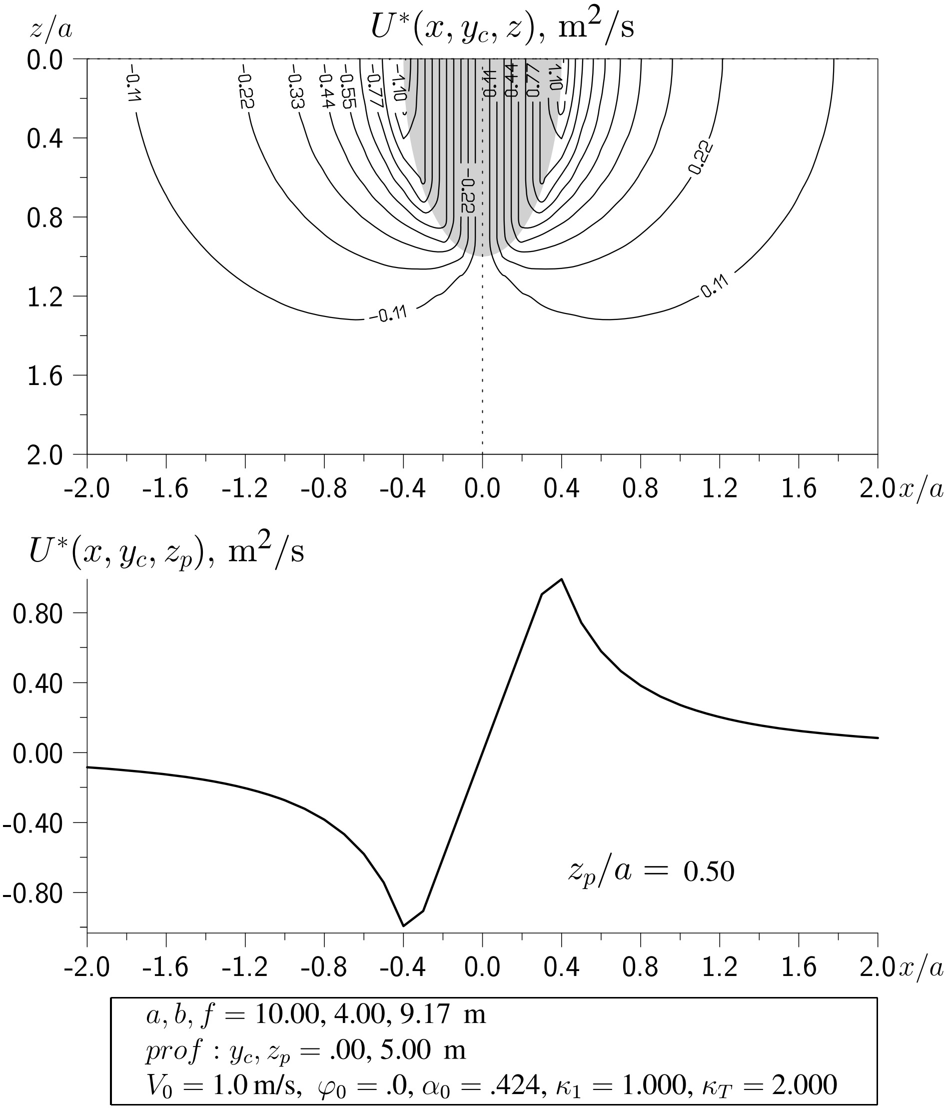

Fig. 2b. Equipotential isolines of the anomalous velocity potential around the prolate hemispheroidal penetrable obstacle. The bottom curve shows the profile at the depth $z_p/a = 0.5$.

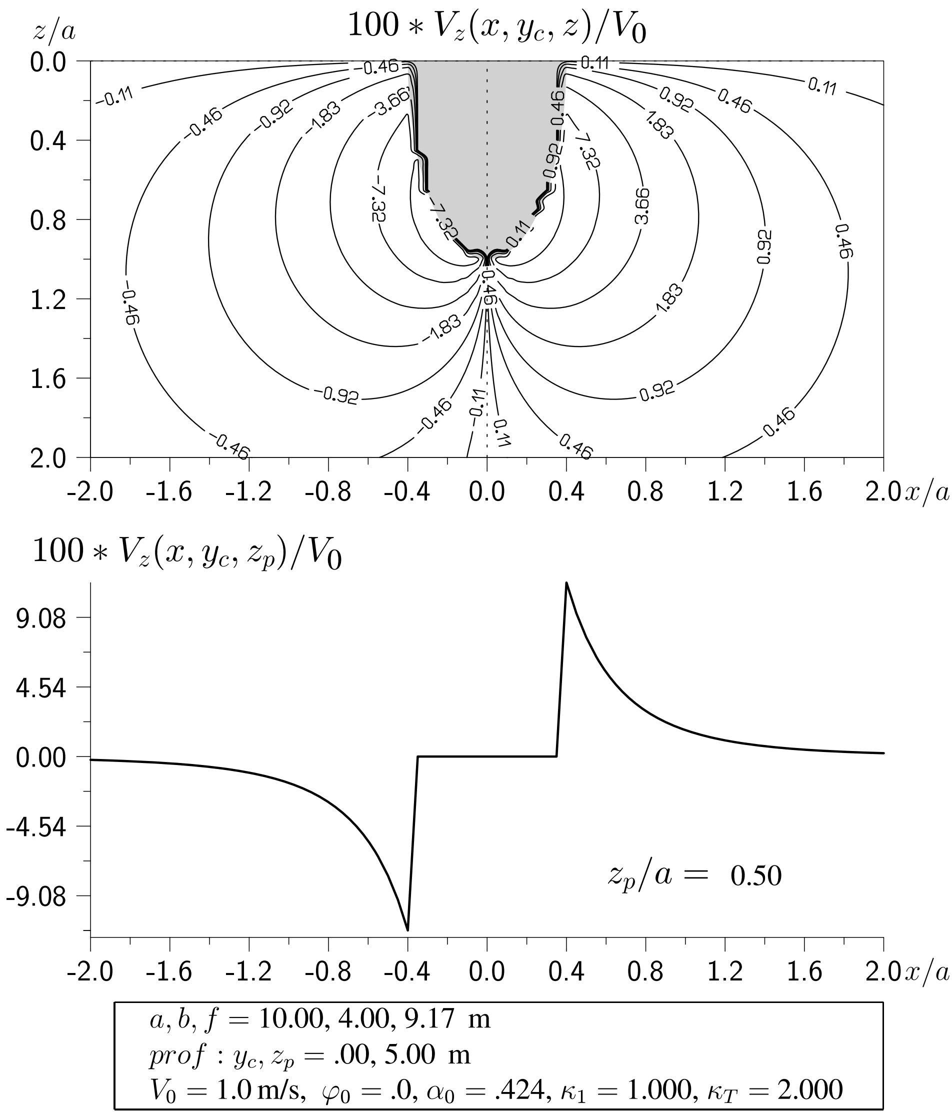

Fig. 2c. Isolines of the vertical (downward) component of the velocity around the prolate hemispheroidal penetrable obstacle. The bottom curve shows the profile at the depth $z_p/a = 0.5$.

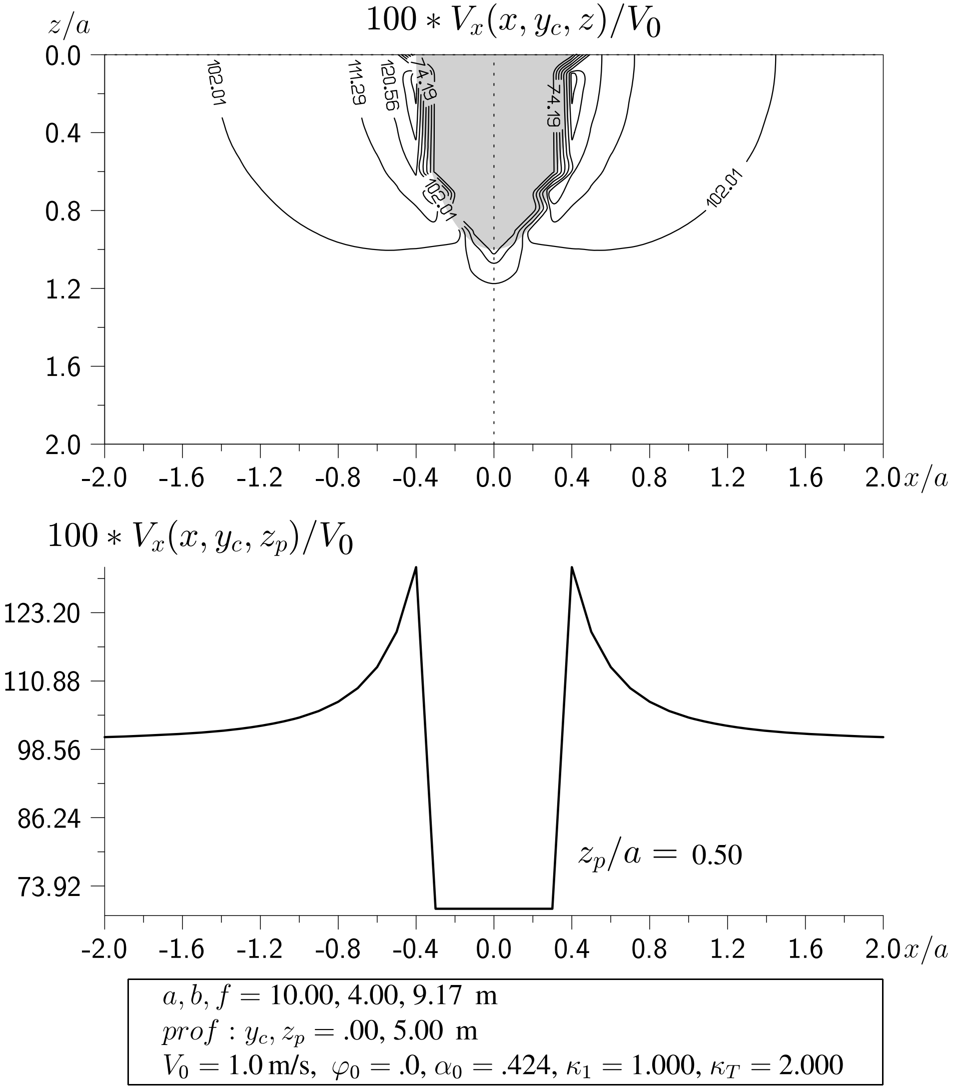

Fig. 2d. Isolines of the horizontal V_x component of the velocity around the prolate hemispheroidal penetrable obstacle. The bottom curve shows the profile at the depth $z_p/a = 0.5$.

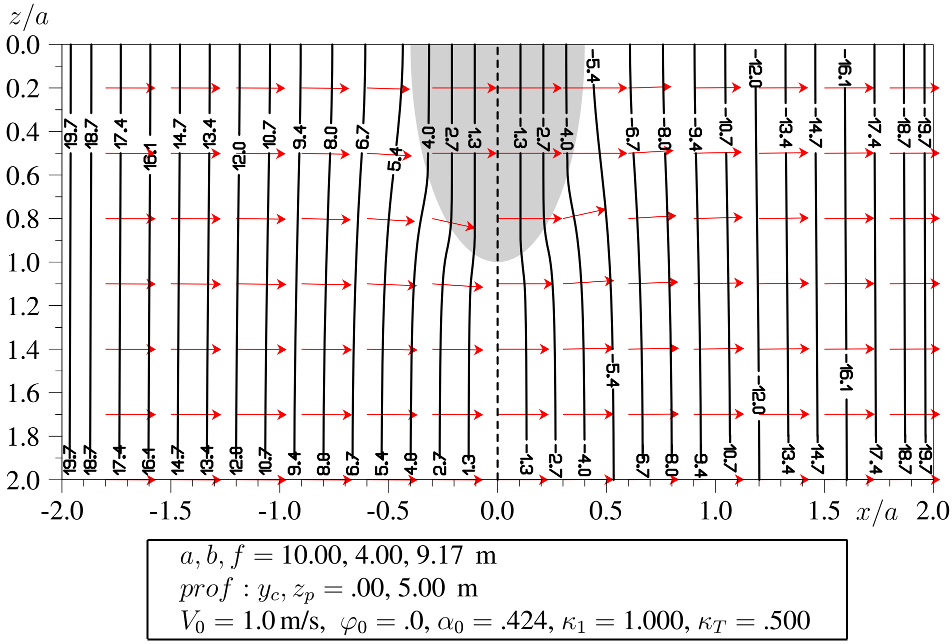

Fig. 3a. Potential isolines around the low-penetrable prolate hemispheroidal obstacle and velocity arrows.

spheroid it drops down to 70%. This jump reflects a discontinuity of the normal component of the velocity, but it is in agreement with continuity of the fluid mass transfer given by $-\kappa\,\mathrm{grad}\,U$. If we multiply the values of V_x by κ_T for $x \in (-b, b)$ the jump for κV_z disappears and we obtain about 45% growth of the groundwater mass inside the most porous halfspheroid ($\kappa_T/\kappa_1 = 2$). It means that we have a good reservoir of groundwater inside this spheroid. We note that in the velocities isoline figures there are quite dense isolines near the boundary of the hemispheroid, which is due to steep changes of the field as showed by the profile curves below. Figure 3a presents the potential lines and velocity vectors for resistive (low porous) halfspheroid ($\kappa_T/\kappa_1 = 0.5$). We see that the stream lines tend to avoid this obstacle. More precisely we can see from Figs 3c–d and the profile curve in Fig. 3d that inside the spheroid there is about 40% deficit in the horizontal groundwater flow $\kappa\,V_x$. This confirms the qualitative differences when

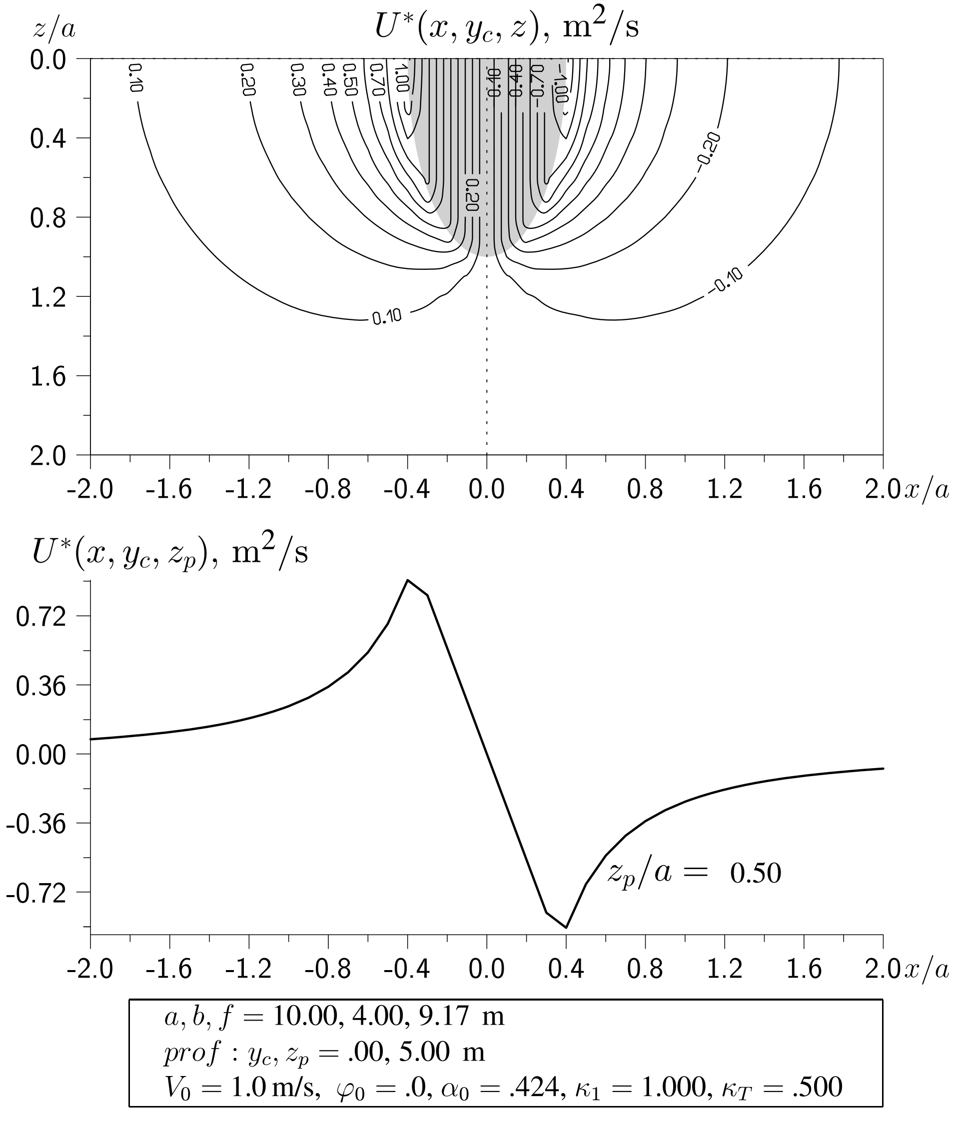

Fig. 3b. Equipotential isolines of the anomalous velocity potential around the prolate hemispheroidal low-penetrable obstacle. The bottom curve shows the profile at the depth $z_p/a = 0.5$.

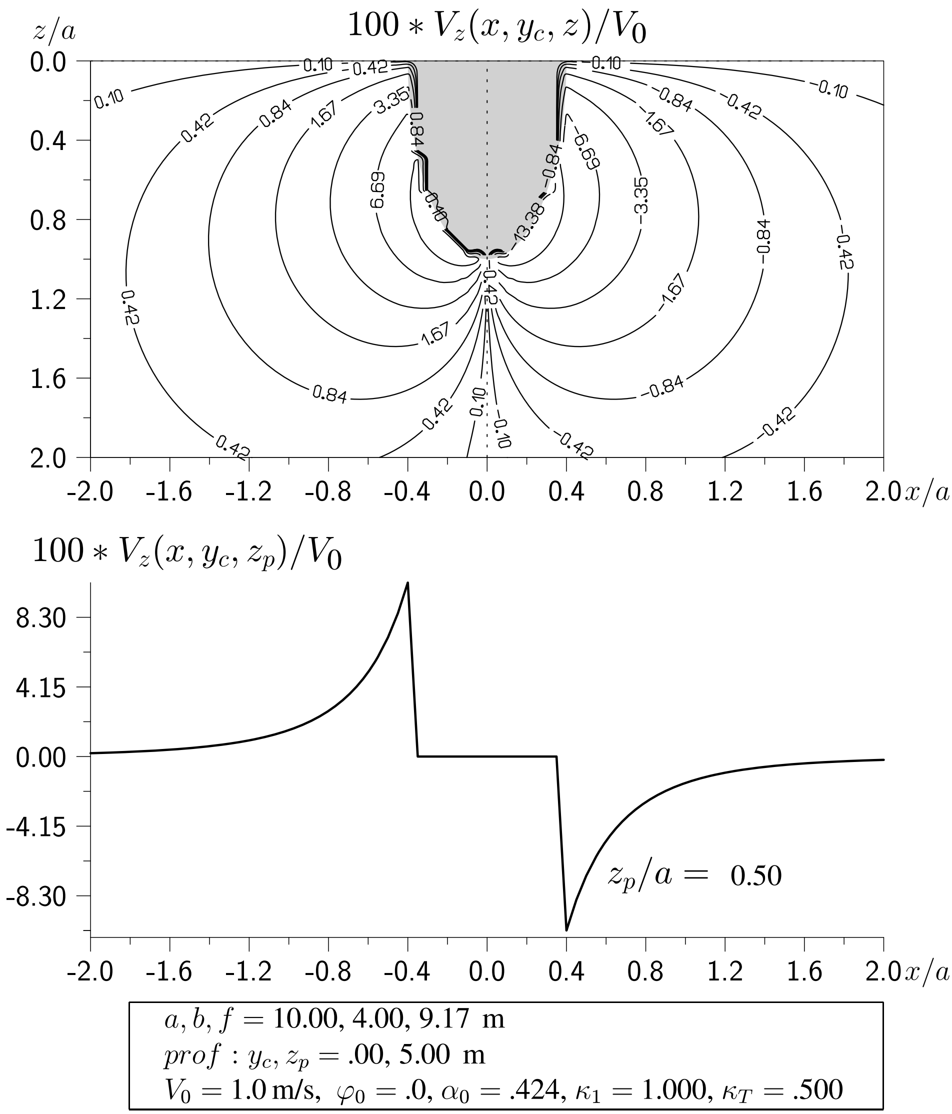

Fig. 3c. Isolines of the vertical (downward) component of the velocity around the prolate hemispheroidal low-penetrable obstacle. The bottom curve shows the profile at the depth $z_p/a = 0.5$.

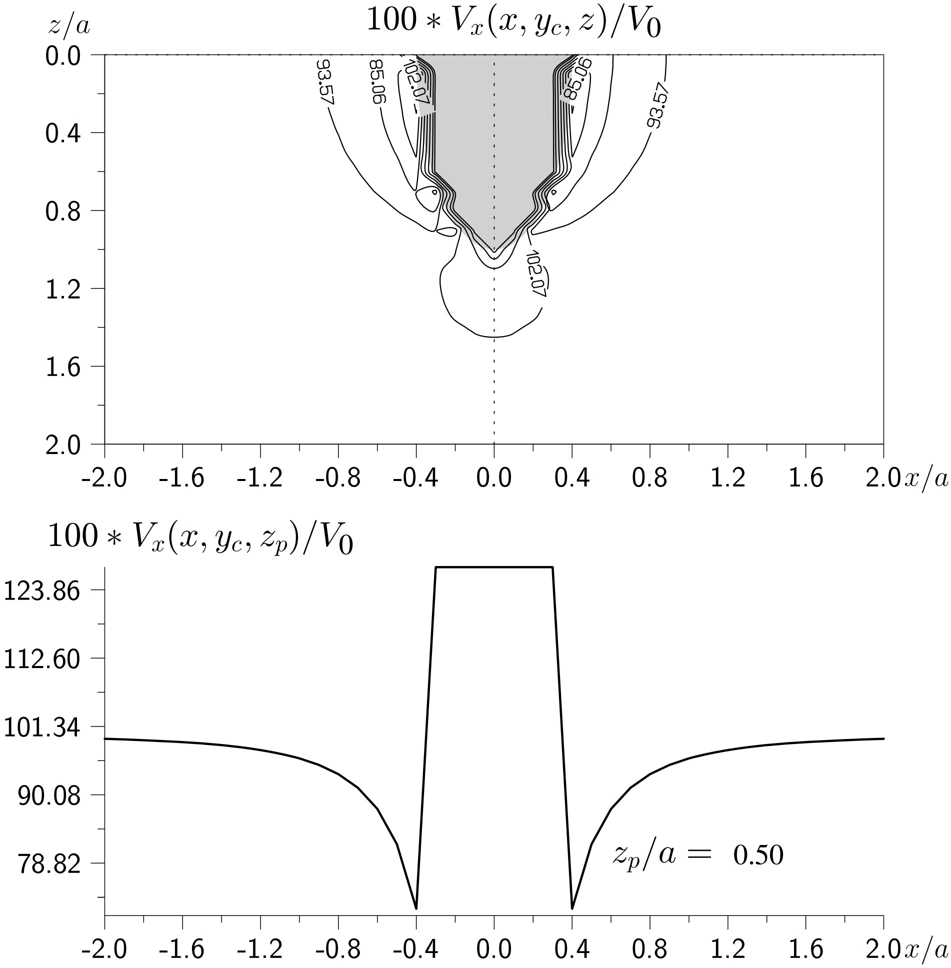

$a, b, f = 10.00, 4.00, 9.17$ m
$prof : y_c, z_p = .00, 5.00$ m
$V_0 = 1.0$ m/s, $\varphi_0 = .0$, $\alpha_0 = .424$, $\kappa_1 = 1.000$, $\kappa_T = .500$

Fig. 3d. Isolines of the horizontal V_x component of the velocity around the prolate hemispheroidal low-penetrable obstacle. The bottom curve shows the profile at the depth $z_p/a = 0.5$.

compared to Figs 2b–d where $\kappa_T/\kappa_1 = 2$.

3. The refraction effect of heat flow due to halfspheroid

Now we will solve the perturbation of the geothermal heat flow due to the prolate hemispheroidal body at the surface of the earth. The unperturbed temperature field in the halfspace $z > 0$ is considered in the form of linear growth with the depth:

$$T_0(z) = E_0\, z, \tag{43}$$

where $E_0 = q_0/\lambda_1$ gives gradient of the temperature, q_0 is the normal heat flow density of about $60\,\mathrm{mW/m^2}$ and λ_1 is the thermal conductivity coefficient of the halfspace outside the hemispheroid. The unperturbed thermal field (43) corresponds to the uniform heat flow density

$$q_0 = \lambda_1\, \partial T_0/\partial z, \tag{44}$$

in the superficial parts of the earth's crust. Now we will determine the perturbation of the uniform temperature field due to the presence of the prolate hemispheroidal body of thermal conductivity λ_T. We will employ an analogy with the groundwater potential problem in the previous section. There is a well-known result that the temperature field in considered region must be a harmonic function. Using the prolate spheroidal coordinates given in (8) we have the unperturbed temperature (43) in the form:

$$T_0(z) = E_0\, z = E_0 f\, \mathrm{ch}\,\alpha \cos\beta. \tag{45}$$

Due to the z-axis symmetry of this field (independent of x, z coordinates) as well as the uniformity of surrounding halfspace, all the temperature field will be independent of the azimuthal coordinate field. Since the β dependence in (45) is given by the $\cos\beta = P_1(\cos\beta)$ it is clear that from the particular solutions (18) will use only terms with $m = 0$ and $n = 1$. Then we will have the temperature field outside of the hemispheroid

$$T_1(\alpha, \beta) = E_0 f \left[\mathrm{ch}\,\alpha + F_1 Q_1(\mathrm{ch}\,\alpha)\right] \cos\beta \tag{46}$$

which satisfies the boundary condition on the surface $z = 0 \equiv \beta = \pi/2$:

$$T_1(\alpha,\beta)|_{\beta=\pi/2} = 0. \tag{47}$$

The temperature field T_2 inside of the hemispheroid is proportional to $T_0(z)$ given by (42), since in solutions of Laplace equation cannot occur functions $Q_1(\mathrm{ch}\,\alpha)$ which are singular on the focal segment $z \in (-f, +f)$. So we have:

$$T_2(\alpha,\beta) = G_2 E_0 f \,\mathrm{ch}\,\alpha \cos\beta. \tag{48}$$

This solution automatically satisfies the condition of zero value at $\beta = \pi/2$. On the surface of the spheroid $\alpha = \alpha_0$, there must be continuity of the temperature field and normal density of the heat flow:

$$[T_1(\alpha,\beta)]_{\alpha_0} = [T_2(\alpha,\beta)]_{\alpha_0}\,, \tag{49}$$

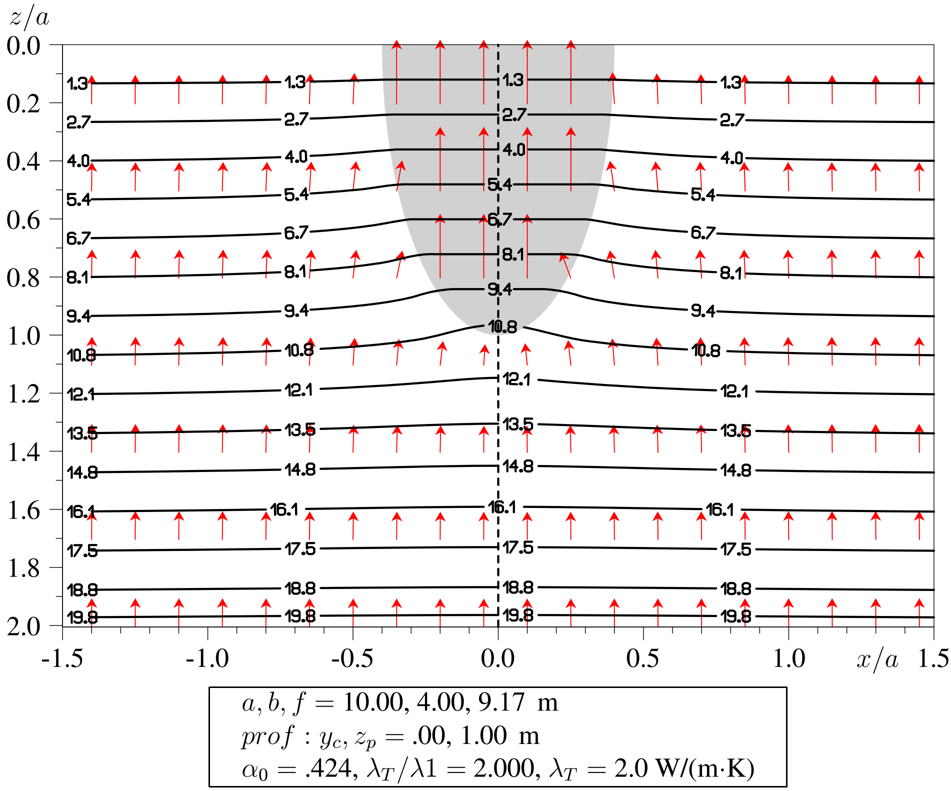

Fig. 4a. Isotherms and heat flow arrows at the hemispheroidal good conductive obstacle.

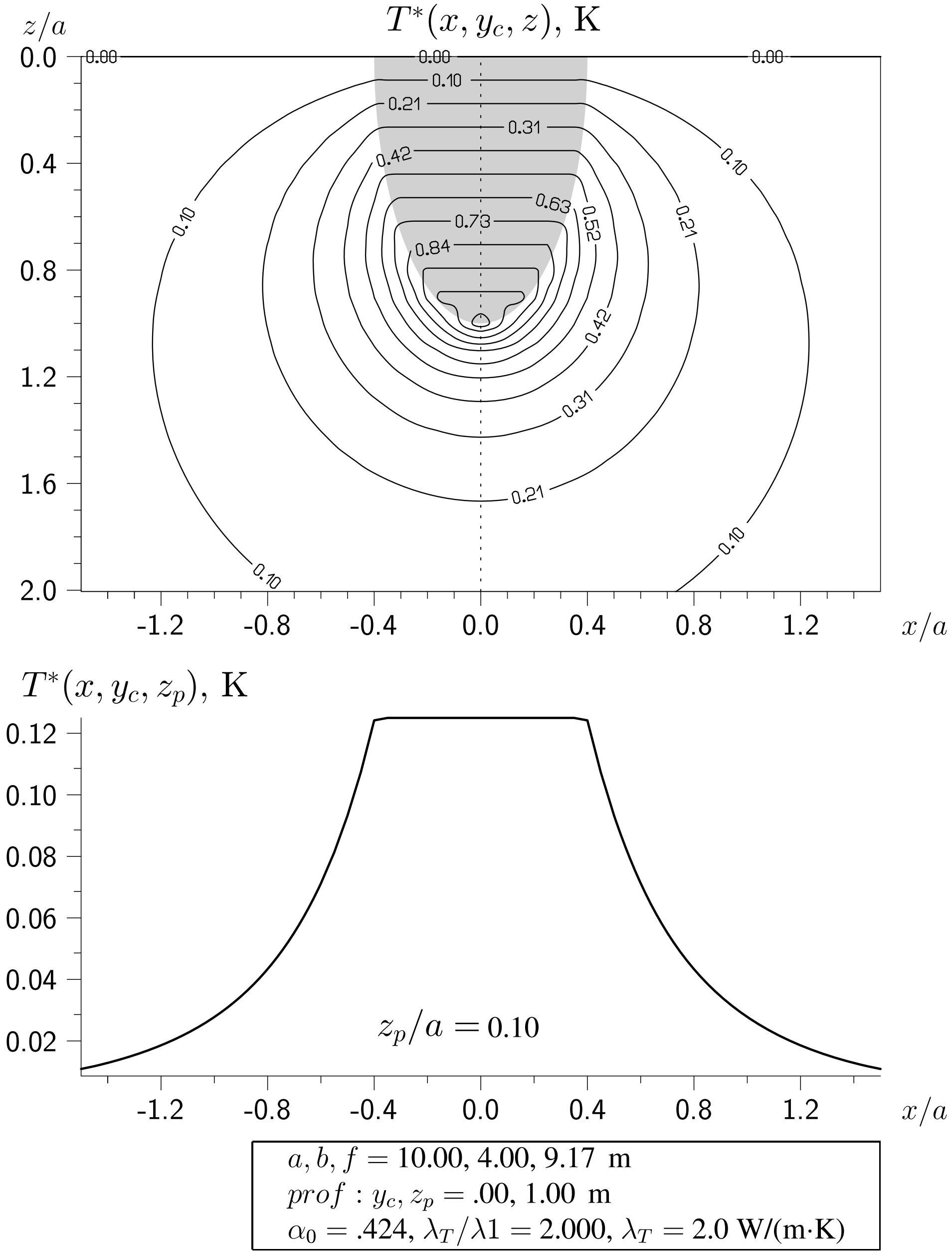

Fig. 4b. Isotherms of the anomalous temperature field around the hemispheroidal good conductive obstacle.

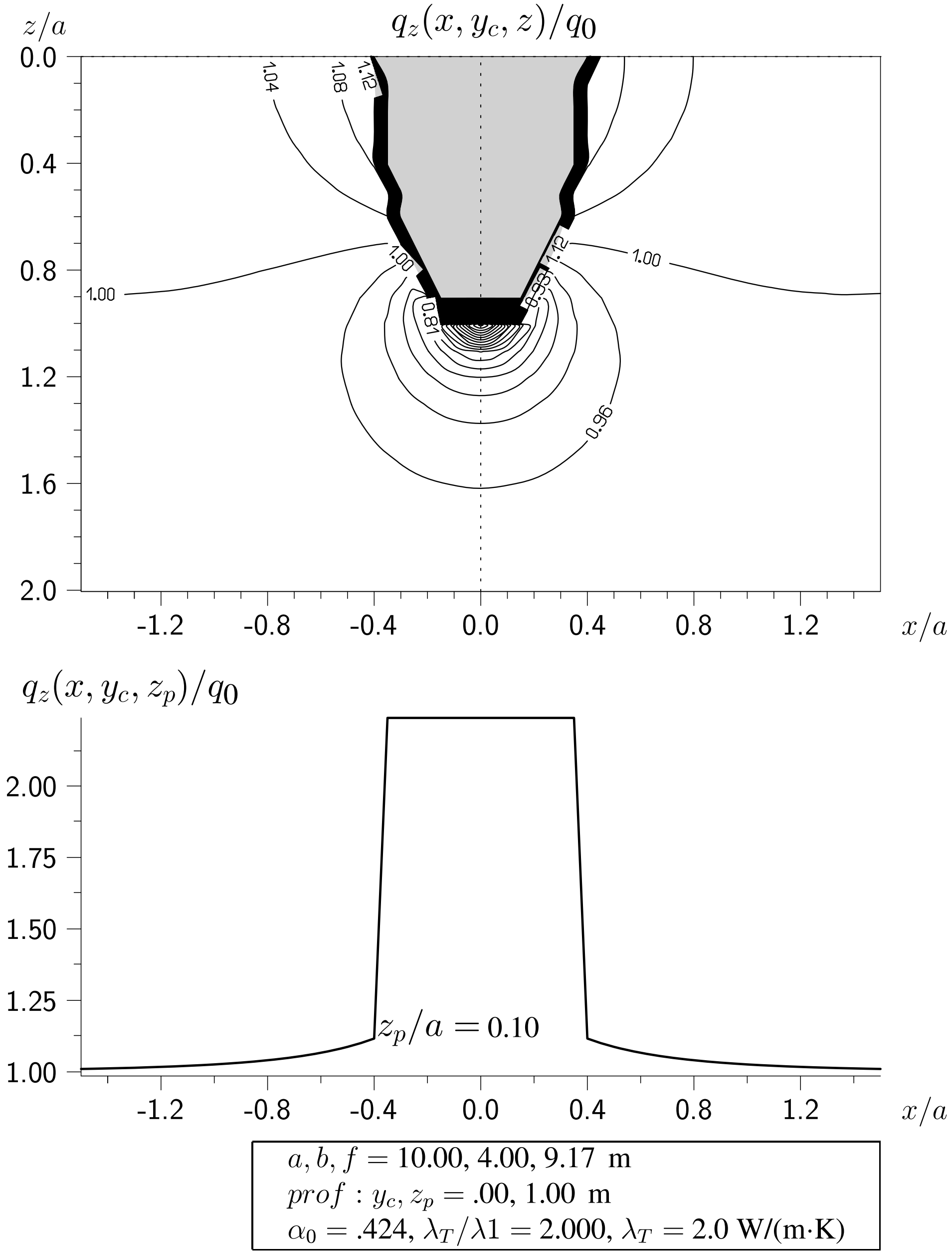

Fig. 4c. Vertical heat flow associated with the anomalous temperature field around the hemispheroidal good conductive obstacle.

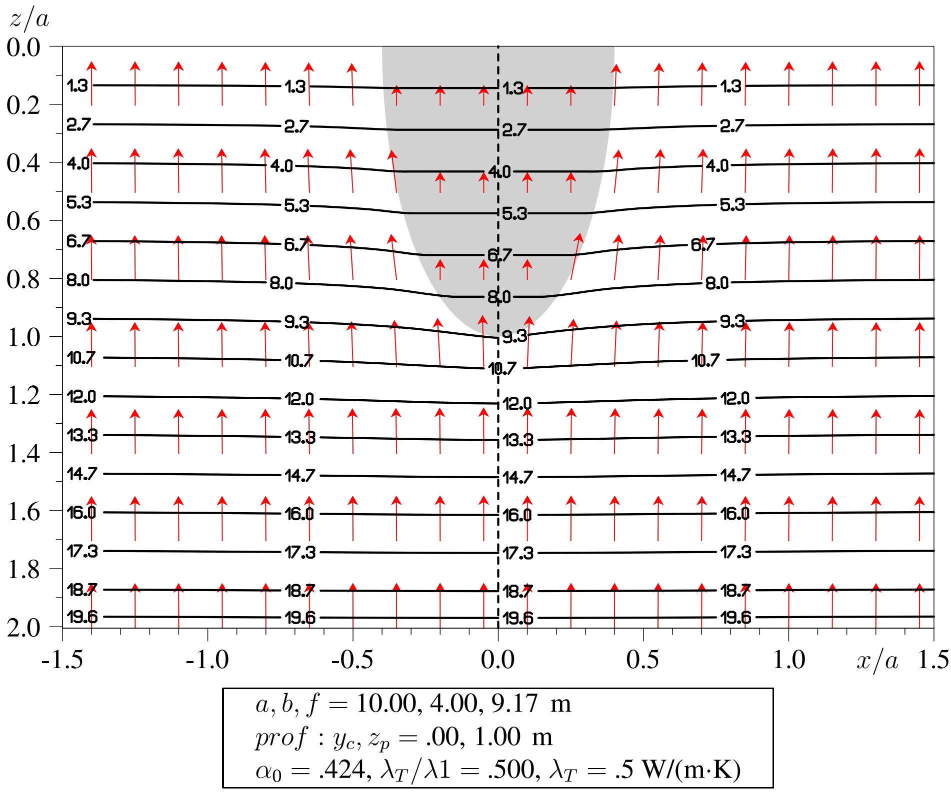

Fig. 5a. Isotherms and heat flow arrows at the hemispheroidal low-conductive obstacle.

$$[\partial T_1(\alpha,\beta)/\partial\alpha]_{\alpha 0} = (\lambda_T/\lambda_1)\,[\partial T_2(\alpha,\beta)/\partial\alpha]\,. \tag{50}$$

Clearly we obtain two equations for F_1 and G_2:

$$\mathrm{ch}\,\alpha_0 + F_1 \cdot Q_1(\mathrm{ch}\,\alpha) = G_2 \cdot \mathrm{ch}\,\alpha_0, \quad 1 + F_1 \cdot Q_1'(\mathrm{ch}\,\alpha_0) = \frac{\lambda_T}{\lambda_1} G_2. \tag{51}$$

By the elimination method we obtain the formulae:

$$F_1 = \frac{(1-\lambda_T/\lambda_1)\,\mathrm{ch}\,\alpha_0}{\mathrm{ch}\,\alpha_0 Q_1'(\mathrm{ch}\,\alpha_0) - (\lambda_T/\lambda_1)Q_1(\mathrm{ch}\,\alpha_0)}, \tag{52}$$

$$G_2 = 1 + \frac{(1-\lambda_T/\lambda_1)Q_1(\mathrm{ch}\,\alpha_0)}{\mathrm{ch}\,\alpha_0 Q_1'(\mathrm{ch}\,\alpha_0) - (\lambda_T/\lambda_1)Q_1(\mathrm{ch}\,\alpha_0)}. \tag{53}$$

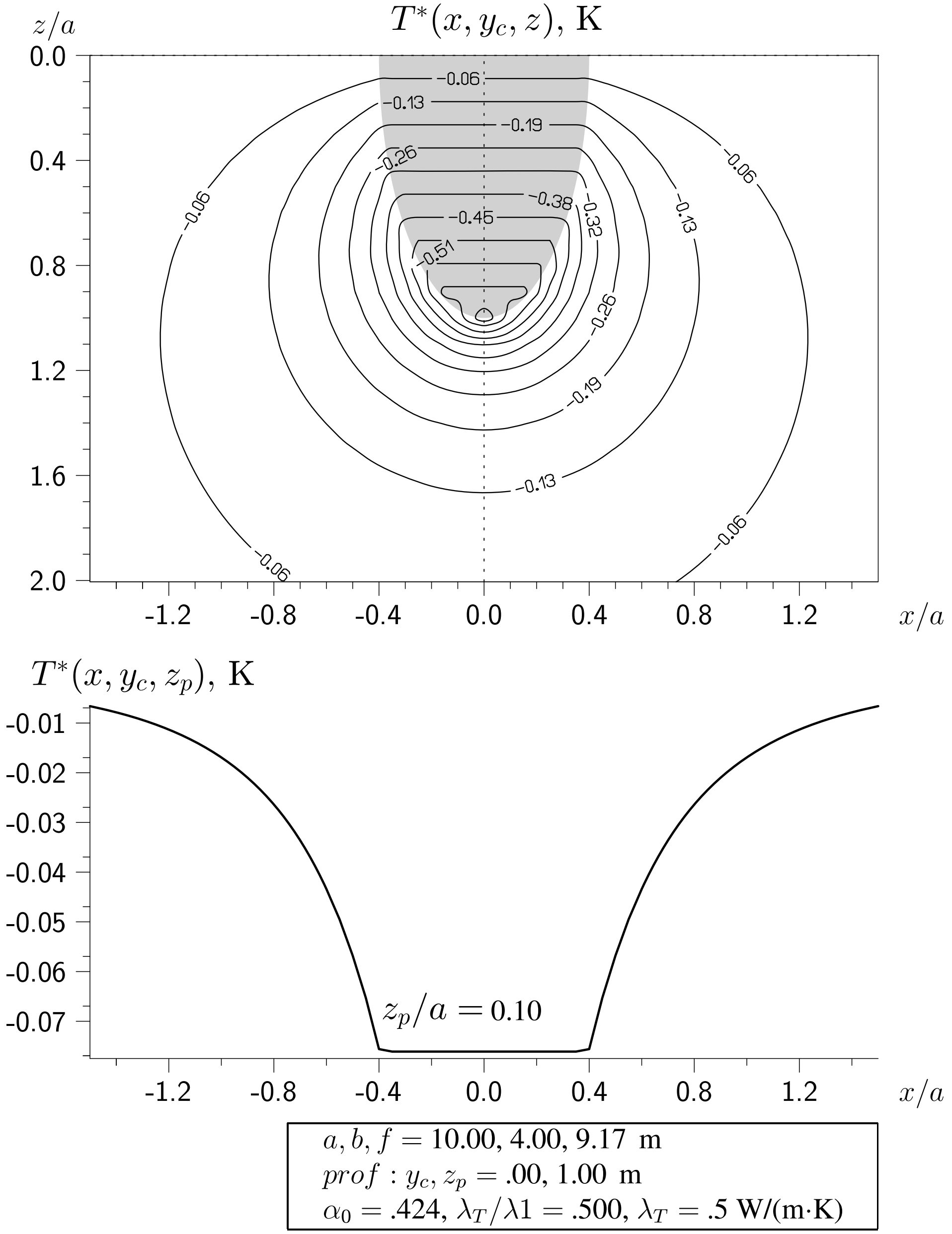

Fig. 5b. Isotherms of the anomalous temperature field around the hemispheroidal low-conductive obstacle.

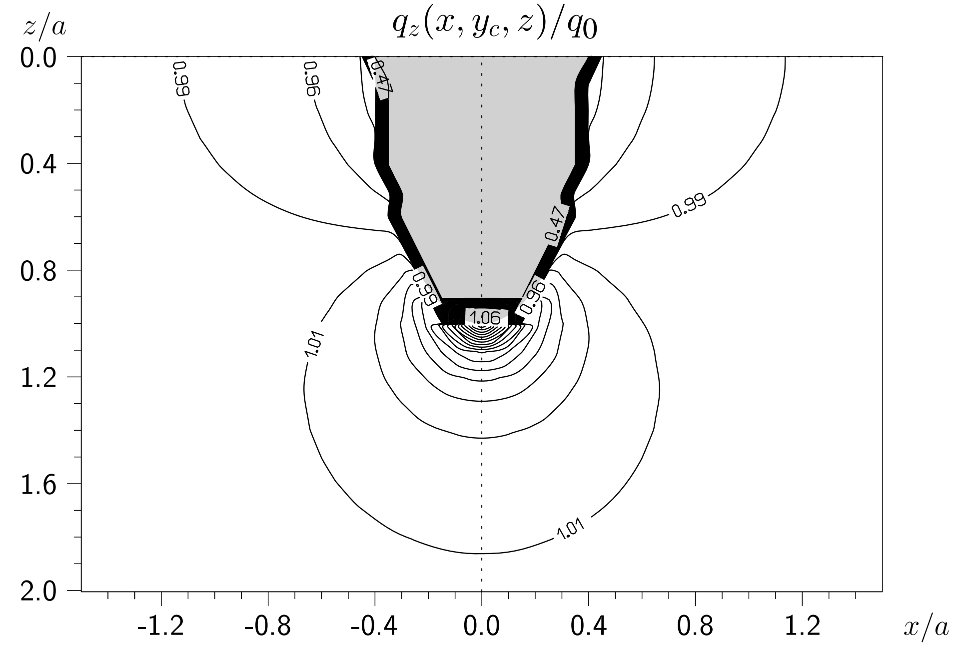

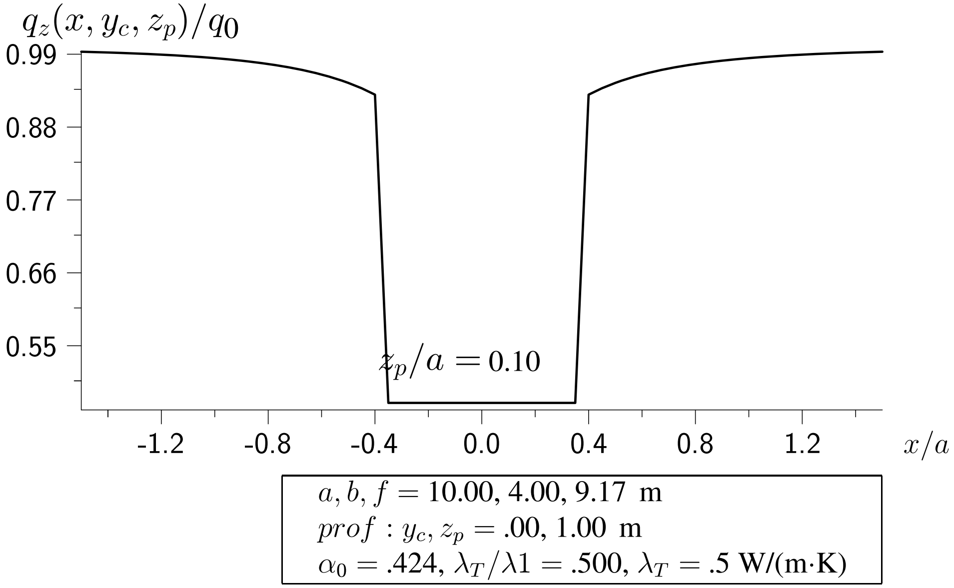

Fig. 5c. Vertical heat flow of the anomalous around the hemispheroidal low-conductive obstacle.

We can easily use these formulae to calculate the temperature field as well as the heat flow. Let us stress that in the geothermics the following formula for the vertical heat flow is used:

$$q_z = \lambda \partial T/\partial z, \tag{54}$$

in contrast to the physical formula $\boldsymbol{q} = -\lambda \operatorname{grad} T$. On the surface of the earth, which corresponds to $\beta = \pi/2$, we have:

$$q_{z2}|_{\beta=\pi/2} = \lambda_T \, G_2 \, E_0, \tag{55}$$

$$q_{z1}|_{\beta=\pi/2} = q_0 + \lambda_1 \, q_{z1}^*, \tag{56}$$

where in analogy with V_z^* the anomalous heat flow density q_{z1}^* outside the hemispheroid is:

$$q_z^* = \left[\frac{1}{h_\beta} \frac{\partial T_1^*}{\partial \beta} \, (\mathrm{sh}^2\alpha + \sin^2\beta)^{-1/2} \right]_{\beta=\pi/2}, \tag{57}$$

where $T_1^* = E_0 f F_1 Q_1(\mathrm{ch}\,\alpha) \cos\beta$ is the anomalous temperature outside the hemispheroid, as determined from (46).

4. Conclusion

Our results from the analytical model calculations clearly show that most perspective places for good groundwater heat wells occur at conditions with increased filtration and thermal conductivity coefficients of the hemispheroid i.e. $\kappa_T/\kappa_1 \geq 2$, $\lambda_T/\lambda_1 \geq 2$. There is necessary at first to determine prevailing direction of the unperturbed groundwater flow far from the hemispheroid and this direction we put as $\varphi_0 = 0$ in application of our theoretical formulae. The presented Figs. 2a–d and Figs. 3a–d are applicable for horizontal direction angle $\varphi = 0$. These wells must be situated on the side of good conductive hemispheroid where $V_z < 0$ i.e. $x/a < 0$, which means groundwater flow towards to the surface or in best condition the well situate near the axis of symmetry of the hemispheroid.

Acknowledgments. The author is grateful to the Slovak Grant Agency VEGA for partial support of the work by means of project No. 2/7008/27.

References

Arfken G., 1966: Mathematical methods for physicists, Academic Press London, 1966.

Bear J., Verruijt A., 1987: Modeling Groundwater Flow and Pollution. D. Reidel Publ. Comp., Dordrecht.

Cook K. L., Van Nostrand R. C., 1954: Interpretation of resistivity data over filled sinks. Geophysics, 19, 761–770.

Hvoždara M., 2005: Geothermal anomaly due to a cylindrical obstacle buried in the halfspace with groundwater flow. Contr. Geophys. Geod., **35**, 2, 113–125.

Hvoždara M., 2008: Groundwater flow anomalies due to an oblate spheroid. Contr. Geophys. Geod., **38**, 1, 61–77.

Madelung E., 1957: Die Mathematischen Hilfsmittel des Physikers. Spriger-Verlag, Berlin.

Morse P. M., Feschbach H., 1973: Methods of theoretical physics. McGraw-Hill Comp. New York.

Lebedev N. N., 1963: Special functions and their applications. Fizmatgiz, Moscow (in Russian).

Smythe W. R., 1968: Static and dynamic electricity. McGraw-Hill, New York.

Wait J. R., 1982: Geo-electromagnetism. Academic Press, New York.